ECOLOGY
ECOLOGICAL SOCIETY OF AMERICA

Seasonality of reproduction in an ever-wet lowland tropical forest in Amazonian Ecuador

Nancy C. Garwood[1] | Margaret R. Metz[2] | Simon A. Queenborough[3,4] |
Viveca Persson[5,6] | S. Joseph Wright[7] | David F. R. P. Burslem[5] |
Milton Zambrano[4] | Renato Valencia[4]

[1]School of Biological Sciences, Life Science II, Southern Illinois University, Carbondale, Illinois, USA

[2]Department of Biology, Lewis & Clark College, Portland, Oregon, USA

[3]Yale School of the Environment, Yale University, New Haven, Connecticut, USA

[4]Laboratorio de Ecología de Plantas, Escuela de Ciencias Biológicas, Pontificia Universidad Católica del Ecuador, Quito, Ecuador

[5]School of Biological Sciences, University of Aberdeen, Aberdeen, UK

[6]Department of Botany, Natural History Museum, London, UK

[7]Smithsonian Tropical Research Institute, Panama City, Panama

Correspondence
Margaret R. Metz
Email: mmetz@lclark.edu

Abstract

Flowering and fruiting phenology have been infrequently studied in the ever-wet hyperdiverse lowland forests of northwestern equatorial Amazonía. These Neotropical forests are typically called aseasonal with reference to climate because they are ever-wet, and it is often assumed they are also aseasonal with respect to phenology. The physiological limits to plant reproduction imposed by water and light availability are difficult to disentangle in seasonal forests because these variables are often temporally correlated, and both are rarely studied together, challenging our understanding of their relative importance as drivers of reproduction. Here we report on the first long-term study (18 years) of flowering and fruiting phenology in a diverse equatorial forest, Yasuní in eastern Ecuador, and the first to include a full suite of on-site monthly climate data. Using twice monthly censuses of 200 traps and >1000 species, we determined whether reproduction at Yasuní is seasonal at the community and species levels and analyzed the relationships between environmental variables and phenology. We also tested the hypothesis that seasonality in phenology, if present, is driven primarily by irradiance. Both the community- and species-level measures demonstrated strong reproductive seasonality at Yasuní. Flowering peaked in September–November and fruiting peaked in March–April, with a strong annual signal for both phenophases. Irradiance and rainfall were also highly seasonal, even though no month on average experienced drought (a month with <100 mm rainfall). Flowering was positively correlated with current or near-current irradiance, supporting our hypothesis that the extra energy available during the period of peak irradiance drives the seasonality of flowering at Yasuní. As Yasuní is representative of lowland ever-wet equatorial forests of northwestern Amazonía, we expect that reproductive phenology will be strongly seasonal throughout this region.

INTRODUCTION

Seasonality is a ubiquitous feature of life on Earth. Organisms synchronize the timing of major life events to match suitable environmental conditions. At temperate and boreal latitudes, reproduction is delimited by a distinct moist and warm growing season with more daylight hours (Delpierre et al., 2016; Morellato et al., 2013; Staggemeier et al., 2020). In contrast, seasons in the tropics are usually defined by variation in rainfall between dry and wet periods (Leigh et al., 1985; Reich, 1995; Richards, 1952; van Schaik et al., 1993; von Humboldt, 1850). Seasonal variation in water and light availability both impose physiological limits on plant phenology in lowland tropical forests because of the turgor pressure needed to expand growing cells and the energy required to fuel photosynthesis (van Schaik et al., 1993; Wright, 1996; Zimmerman et al., 2007).

The search for the drivers of reproductive phenology in the tropics is plagued by the challenge of separating drivers (ultimate causes) of phenology from the cues (proximate causes) used to time reproduction, by temporal correlations among the most likely environmental variables such as water and irradiance, by the incompleteness of climate data, and by the short-term nature of most studies. In addition, the different stages of reproduction (phenophases), from flowering through fruit development, seed dispersal, seed germination, and seedling establishment, may respond to different environmental or biotic drivers. For example, long periods of heavy rainfall might impede insect pollination but promote seed germination. Later phenophases are dependent on the success of previous phases.

A recent review of 218 phenological studies in the Neotropics (Mendoza et al., 2017) found that most studies were conducted in seasonal sites with a distinct dry season that places physiological limits on plant activity and leaves the role of irradiance underappreciated. Most studies were also short term (only 10 included >10 years of observations), which may have missed subtle seasonal patterns if they are hidden by interannual variation. In short-term studies of seasonal sites, it is difficult to separate the relative effects of irradiance, daylength, and water availability because they are highly correlated. Importantly, only seven of the reviewed studies measured irradiance, a proposed key driver of reproduction (Mendoza et al., 2017).

Examining the phenology of lowland ever-wet forests at low latitudes can help to disentangle potential environmental drivers that are correlated elsewhere. First, ever-wet forests lack a distinctive and predictable dry season, so precipitation should always exceed potential evapotranspiration (Whitmore, 1984), lessening the physiological constraints of water limitation on phenology (Wright, 1996). Second, equatorial forests isolate the effect of irradiance (the intensity of solar radiation) from daylength (the duration of solar radiation). Daylength varies by only a few minutes on the equator and thus has a negligible effect on seasonal variation in daily radiation in equatorial forests. In addition, given the minimal seasonal change in daylength, it is unlikely to be a major proximate cue for reproduction (unlike its role at higher latitudes), making it easier to identify the ultimate drivers of phenology. Top-of-atmosphere irradiance varies seasonally, depending on the angle and distance from the Sun at each latitude, and is bimodal at equatorial latitudes (McGregor & Nieuwolt, 1998), making it a potentially important driver and proximate cue of reproduction. What plants experience, however, is the irradiance received at the Earth's surface or top of the forest, which is lower than top-of-atmosphere radiation due to impacts of clouds, dust, and pollution. The modality of top-of-forest irradiance will depend on the seasonality of cloudiness.

The few long-term studies of tropical phenology that measured irradiance have suggested that reproduction tracks the seasonality of top-of-forest irradiance (Chang-Yang et al., 2013; Zimmerman et al., 2007). Extreme El Niño dry seasons produce prolonged periods of reduced cloudiness that increase tree reproduction (Ashton et al., 1988; Wright & Calderón, 2006) and alter growth patterns (Hogan et al., 2019). However, the driest months do not always coincide with the period of greatest irradiance: in much of western tropical Africa light availability actually peaks during the rainy season due to cloudy dry seasons (Wright & van Schaik, 1994). Photosynthesis in some tropical trees is often limited by light (Graham, 2003; Huete et al., 2006; Wu et al., 2017), which might select for growth or reproduction during seasons of higher irradiance.

The idea that tropical rain forests are stable environments with a climate that does not vary in predictable annual patterns (Borchert et al., 2015; Calle et al., 2010) persists in a large part because there is a dearth of local climate information from locations thought to be the least seasonal (Neill & Jørgensen, 1999). Only four of the 218 Neotropical studies reviewed by Mendoza et al. (2017) were from the equatorial forests of northwestern Amazonía. In the lowland Amazon basin, the equatorial

northwest is considered the wettest and least seasonal region, whereas equatorial sites further east have distinct dry seasons and single annual peaks of high rainfall, and nonequatorial sites to the southwest have lower but bimodal rainfall (Espinoza Villar et al., 2009; Leigh Jr., 2004; Silman, 2011; Sombroek, 2001; Xiao et al., 2006). Whether subtle seasonal changes in environmental parameters in the least seasonal Amazonian sites drive seasonal reproduction is largely unexplored. Understanding climatic effects on reproduction in this region is essential for predicting changes in reproduction as climate changes.

To disentangle the effects of light and other environmental variables on tropical phenology, we initiated a study in 2000 in the equatorial lowland tropical rain forest of Yasuní National Park, Ecuador (Persson, 2005), located in the wettest and least seasonal region of the Amazon basin (Silman, 2011; Xiao et al., 2006). Yasuní receives ~3000 mm of rainfall annually, no month on average is dry (<100 mm rainfall), and seasonal temperature fluctuations are small, based on a 53-month record (Pitman, 2000; Valencia, Condit, Romoleroux, et al., 2004; Valencia, Foster, Villa, et al., 2004). Daylength varies by just 9 min over the year, but irradiance had never been measured. Here we present an 18-year-long community-level phenological dataset of flowering and fruiting, which includes more than 1500 taxa from diverse lifeforms, coupled with on-site climate data, including top-of-forest irradiance, over the same period. We addressed four questions concerning the relationships between phenology and environmental variables. (1) Is there predictable seasonal variation in the reproductive activity of plants in an ever-wet equatorial forest? (2) What is the amplitude and seasonality of potential environmental drivers in such sites? (3) Does variation in reproductive activity track variation in the potential environmental drivers, specifically top-of-forest irradiance? (4) Do flowering and fruiting phenophases track the same or different drivers? We expected some level of seasonality of irradiance and phenology and predicted that reproductive activity at Yasuní would be greatest during periods of high top-of-forest irradiance.

METHODS

Study site

Estación Científica Yasuní (ECY, 0°41′ S, 76°24′ W), administered by Pontificia Universidad Católica del Ecuador, lies within Yasuní National Park. The park and the adjacent Huaorani Ethnic Reserve together represent the largest conserved area (1.6 m ha) of mature forest in the Ecuadorian Amazon (Valencia, Condit, Romoleroux, et al., 2004). The park has an elevation ~200 m above sea level (asl). The dominant vegetation type is evergreen terra firme forest, with a canopy height of 15–30 m and emergent trees reaching 50 m (Valencia, Foster, Villa, et al., 2004).

We worked in the 50-ha Yasuní Forest Dynamics Plot (YFDP), established in 1995, wherein all trees ≥1 cm diameter at 1.3 m height are mapped, tagged, measured, and identified approximately every 5 years (Valencia, Condit, Romoleroux, et al., 2004; Valencia, Foster, Villa, et al., 2004). The YFDP is hyperdiverse, with 1104 species recorded in the initial census of the first 25 ha (Valencia, Condit, Romoleroux, et al., 2004), and has high familial and generic tree diversity, with more than 40 species of *Inga* (Fabaceae) and *Miconia* (Melastomataceae) and 16 species of Myristicaceae coexisting in this plot (Queenborough et al., 2007; Valencia, Condit, Romoleroux, et al., 2004). See Valencia, Condit, Romoleroux, et al. (2004), Valencia, Foster, Villa, et al. (2004) for further information on the YFDP and Netherly (1997) for paleohistory.

The climate of Yasuní has been described as "aseasonal" (Perez et al., 2014; Valencia, Condit, Foster, et al., 2004) because mean annual rainfall (3081 mm) and mean monthly rainfall (174–412 mm) are high, no month on average is dry (i.e., <100 mm), and the mean monthly minimum (21.2–23.4°C) and maximum (33.7–36.6°C) temperatures are relatively constant (Valencia, Condit, Foster, et al., 2004). Rainfall in the wider region, however, does vary throughout the year, with an April–May peak larger than an October–November peak (Pitman, 2000; Valencia, Foster, Villa, et al., 2004).

Reproductive data

We monitored community-level flowering and fruiting activity using the methods of Wright and Calderón (1995) for Barro Colorado Island, Panama, and a network of 200 traps that caught any plant material that fell from above. Each trap is a 0.75×0.75 m^2 (0.57 m^2) of 1 mm fiberglass wire mesh, supported by PVC and raised 0.75 m off the ground. Traps were stratified along the trail system throughout the YFDP (see Appendix S1: Section S1 for a description of the 200 traps and their position).

Traps were examined approximately every 2 weeks (a "census") from February 2000 to February 2018 (censuses 1–435). In each census, all reproductive parts in traps were counted individually and identified (Garwood et al., 2023). For this study, we used only species presence data. Thus, we defined a flower or fruit record as the presence of any number of plant parts of one species in one trap in one census. For this analysis, hermaphroditic, female, or male flower records were combined into a single "flower presence" record for each trap, census, and species.

Similarly, mature seeds, mature fruit, or mature fruit segments (e.g., capsule valves) were combined into a single "fruit presence" record for each trap, census, and species.

Each morphospecies was assigned a unique code and identified as taxonomic species whenever possible, using local reproductive adults and our permanent reference collection. Approximately 1550 morphospecies were recorded across all censuses. Many of these were rare, but 563 species occurred in ≥5 traps and had ≥10 records in 18 years and are the focus of our analyses. Taxa include canopy trees, subcanopy trees, shrubs, lianas, vines, hemi-epiphytes, epiphytes, and terrestrial herbs, so the data provide a sample of the entire forest community.

Environmental data

We compiled our climate data from several different environmental monitoring efforts at Yasuní (Garwood et al., 2023). All equipment was located in the laboratory clearing, away from buildings and vegetation, and placed at a height of 1.5–3 m. These open-sky data from the laboratory clearing are reasonable estimates of top-of-forest conditions, as the average canopy height is ~30 m. We use the term "top-of-forest irradiance" to distinguish our measurements from top-of-atmosphere irradiance, which is measured ~100 km above the surface (https://earthobservatory.nasa.gov/images/7373/the-top-of-the-atmosphere).

First, we measured temperature, rainfall, and solar radiation at ECY from May 2000 to February 2012 with two Li-Cor LI-200S pyranometers (calibrated for the daylight spectrum, 400 to 1100 nm), an LI-1400-102 air temperature sensor, an LI-1400-106 tipping bucket, and an Li-1400 data logger (Li-Cor, Inc., Lincoln, Nebraska, USA). These data were recorded at hourly intervals. This equipment was replaced in 2012 by ECY staff as part of a TEAM (Tropical Ecology Assessment and Monitoring) project. They installed a Campbell Scientific CR1000 data logger, two Vaisala HMP45C and one Rotronic HC2-S3 temperature/relative humidity sensors, a Hydrological Services TB4 precipitation gauge, two LI-COR LI-200X pyranometers (calibrated for the daylight spectrum, 400–1100 nm). This second effort was recorded at 5-min intervals from January 2012 until February 2018. All sensors were calibrated before use and replaced with calibrated sensors when needed to ensure consistency. Daily rainfall data were also collected with a manual rain gauge from 2012 to 2018 by the TEAM project. Appendix S1: Section S2 provides details on data collection, compilation, and cleaning.

We examined regional rainfall using 13 sites in eastern Ecuador to determine whether rainfall seasonality measured at ECY was similar to that of other stations in the region (Appendix S1: Figure S9). These data had record lengths between 6 and 55 years and were used to calculate the mean (±SE) monthly rainfall and annual total rainfall. Last, we compared climate data from ECY to modeled climate data using CRU Ts 4.04 (Climatic Research Unit gridded time series, Version 4.04) for the 0.5 × 0.5 degree pixel that includes the ECY (Anderson-Teixeira et al., 2020; Harris et al., 2020; see Appendix S1: Figures S10–S12).

Data analysis

Reproductive phenology

To document reproductive activity over the 18-year period, we created the phenology time series by counting the total number of species observed across all 200 traps in each month for each phenophase. To summarize community-level phenological activity, we calculated the mean number of species flowering and fruiting for each of the 12 months throughout the year. We also examined temporal patterns in community-level reproductive phenology at Yasuní over the full 18-year time series by testing for autocorrelation at monthly lags for flowering and fruiting. We cross-correlated monthly numbers of species flowering and fruiting over 18 years to examine expected links between flowering and fruiting. Autocorrelations and cross-correlations were conducted on the total number of species present per month using Systat Version 13.1 (Systat Software Inc., 2009).

At the species level, we summarized each species' reproductive phenology using vector algebra, looking at the distributions of vector angles as well as binning these angles into counts of reproductive activity per month (Chang-Yang et al., 2013; Morellato et al., 2010; Zimmerman et al., 2007). Linear analyses are not appropriate for most phenology studies because the seasonal timing data are circular (Batschelet, 1981; Staggemeier et al., 2020). The angle and length of the mean vector of each species were calculated using the software Oriana 4.02 (Kovach, 1994) using the presence (not abundance) of a species in each trap, pooling data from all years together. Angle of the mean vector represents the mean date of reproductive activity (where 0° represents 1 January). The mean vector length (0 to 1) measures the clustering of records around the mean date (where 0 represents continuous reproductive activity and 1 represents highly synchronized reproductive activity occurring on the same calendar day each year). This analysis included only species found in ≥5 traps and represented by ≥50 records (see Appendix S1: Figures S17 and S18 for results of using other cut-off points for sample size). Morphospecies that might include multiple species (e.g., "Piperaceae spp.") were also excluded. To estimate

fruit development time, we determined the midpoint between flowering and seed dispersal by calculating the difference (in days) between the angles of the mean flowering and mean fruiting vectors for species that had ≥50 records for both phenophases. This will underestimate development time in species that require >1 year to complete development.

We analyzed distributions of these vector data in two main ways to detect seasonality in reproduction: (1) at the species level, we compared distributions to a null hypothesis of uniform reproductive activity throughout the year; and (2) at the community level, we examined the distribution of species' mean dates of phenological activity. We asked if reproductive activity departed from the null hypothesis of temporal uniformity using a Rayleigh test (Kovach, 1994; Morellato et al., 2010). Departure from uniformity occurs due to intra-annual or interannual sources of variance that produce many possible distributions around peak periods of reproduction (e.g., unimodal or multimodal distributions), and these departures affect vector lengths. One common potential unimodal distribution indicating a consistent annual peak in reproductive activity is the circular normal (or von Mises) distribution, which we examined for each species using a Kuiper test (Kovach, 1994; Morellato et al., 2010). Other departures from both the uniform and the circular normal distribution (i.e., significant Rayleigh and Kuiper tests) occur through bimodal or multimodal peaks in phenology, a skewed distribution with a long tail, interannual variation in the calendar date of peak reproductive activity, among other possibilities, which we did not explicitly test for. We binned species into four groups according to the results of the Rayleigh and Kuiper tests. The Rayleigh and Kuiper tests were carried out in Oriana 4.02 (Kovach, 1994, 2013). We examined the community-level distribution in mean dates of phenological activity by counting the number of species whose mean reproductive date (i.e., mean vector angle) fell within each calendar month, weighting all species equally, and producing a histogram. Finally, we calculated a single community-wide mean vector angle by calculating the mean vector angle of all the species' mean vector angles. We also calculated a mean of species means for subsets of species whose phenology fit a circular normal and/or nonuniform distribution.

Climate seasonality

We calculated two seasonal variables for Yasuní that are nearly invariant across years (Appendix S1: Section S2.1): solar angle and daylength. The cosine of the solar zenith angle is an indirect measure of potential top-of-atmosphere solar radiation, the driver of global and local climate (Hartmann, 2015). We present daylength, a cue widely used by plants to initiate reproduction in nonequatorial regions, to demonstrate that it scarcely varies throughout the year at Yasuní.

Then we established the observed variation in top-of-forest irradiance, rainfall, temperature, and humidity at Yasuní using the open-sky daily environmental data described above. From the daily Yasuní climate data, we calculated mean monthly values for all climate variables and the correlations among all variables for the 18-year study period based on actual data of months with at least 15 days of data. Sample sizes for individual months were less than the maximum possible (18 months; $N = 11-16$ for irradiance, $N = 11-15$ for rainfall and temperature, and $N = 6-9$ for humidity, which was first recorded in 2008) because of equipment problems. To create a continuous monthly climate record for auto- and cross-correlation analysis, missing monthly data were replaced by the calculated mean for that month based on actual data from 2000 to 2018 (see Appendix S1: Figure S5 which shows actual recorded data and estimated data). As noted above, the dearth of directly observed climate data (and complete lack of irradiance data) from elsewhere in this region makes it impossible to estimate missing data from nearby weather stations or satellite-modeled data (Appendix S1: Sections S3.4 and S3.5).

To detect annual trends in environmental factors at Yasuní, we autocorrelated each factor in the continuous data set (2000–2018), which includes the estimated monthly values for missing monthly data, at monthly lags using Systat 13.1 (Systat Software Inc., 2009). Significant autocorrelation at lag 1 indicates that the value in that month is highly correlated with the value of the previous month; significant autocorrelation at lag 12 indicates that the value in each month is highly correlated with the same month the previous year.

Linking climate and phenology

To test if community-level phenology tracks environmental correlates at Yasuní, we ran cross-correlation analyses between the study-long time series for both flowering and fruiting and each environmental variable in Systat 13.1 (Systat Software Inc., 2009). Two variables with strong annual signals are expected to be significantly cross-correlated; the analysis identifies whether the highest correlations occur in the same time period (lag = 0) or following lags of one or more months. If light levels limit community-wide reproduction, we predicted that the number of species reproducing each month would be positively related to top-of-forest irradiance at short time lags. If moisture availability limits

community-wide reproduction, we predicted that the number of species exhibiting peak reproductive activity would track rainfall.

At the species level, we used contingency table analysis to compare the number of species whose vector angle fell in four 3-month irradiance periods. Using our measured irradiance data, we identified periods of highest irradiance (August–October), intermediate irradiance (November–January) and low irradiance (February–April and May–July). We tested the distribution of species against a uniform distribution, calculating the log-likelihood ratio (G-statistic sensu Sokal & Rohlf, 1995) and carried out a posteriori comparisons using critical values of the chi-square distribution based on Šidák's multiplicative inequality (Table E in Rohlf & Sokal, 1995). We used contingency table analysis to determine whether the midpoints of fruit development time fell in the period of maximum irradiance (August–October).

RESULTS

Strong seasonality in flowering and fruiting patterns

The plant community at Yasuní showed strong and consistent annual patterns in the timing of reproduction in both the total number of species per month across the 18 years of the study (Figure 1) and the mean number of species per month (Figure 2a). Autocorrelations of the number of species flowering and fruiting (Appendix S1: Figure S3) over 18 years were positive and significant at 12-, 24- and 36-month intervals; only coefficients at very

short time lags (1–2 months) were higher than these annual signals. This annual peak in activity for each phenophase clearly demonstrates a strong seasonal component to reproduction in this ever-wet "aseasonal" equatorial forest.

In the annual cycle of peaks and troughs in flowering and fruiting (Figures 1 and 2a), the peaks had nearly 50% more species than the troughs (Figure 2a). Yet, there were also many species flowering or fruiting every month (Figures 1 and 2a). For flowering, the lowest mean number of species flowering occurred in April (82 ± 6.1 species, mean $\pm$ SE), and May (82 ± 4.4), and the highest in September (137 ± 5.7) and October (147 ± 5.1). (Each mean is based on $N = 18$ months, i.e., 18 Aprils, in the 18-year reproductive data set.) For fruiting, the lowest mean number of species fruiting occurred in September (99 ± 4.7) and October (100 ± 2.6) and the highest in March (144 ± 6.0 species) and April (140 ± 5.5). This pattern was also illustrated by individual species, such as *Otoba glycycarpa*, that consistently flowered during the community-level peak each year and fruited some months later (Appendix S1: Figure S16).

The vector analysis of species-level mean dates of reproduction across all species (Figure 3) also showed distinct annual patterns in reproduction at the community level (Garwood et al., 2023). For flowering (224 species), the greatest number of mean vector angles (the average time of reproduction) occurred in October and November (Figure 3b), overlapping the period identified as peak flowering in the species-count community analysis above (August–October; Figure 2a). For fruiting (271 species), the greatest number of mean vector angles occurred in February and March (Figure 3e), again
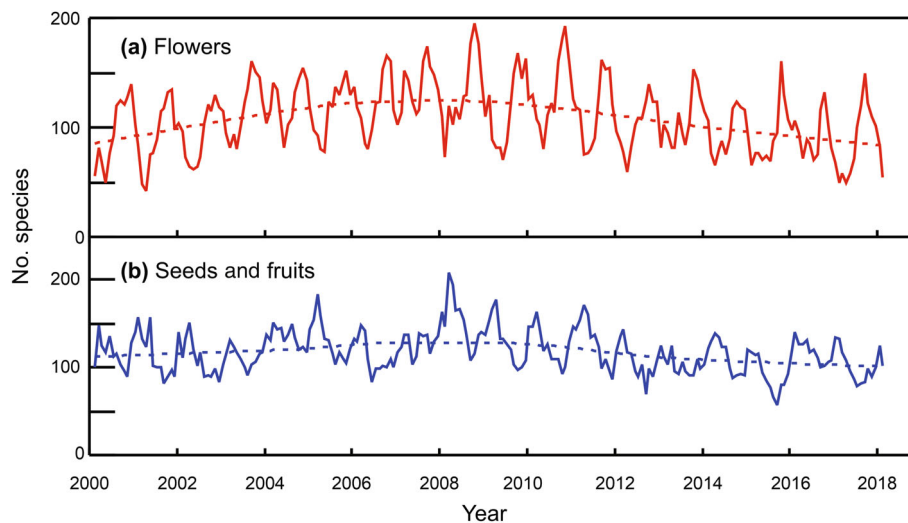

FIGURE 1   Community-level reproductive activity at Yasuní. Total number of species reproducing per month from February 2000 to February 2018 in all 200 traps. (a) Flowers and (b) seeds and/or mature fruit. Dashed line is the Lowess fit to the data.
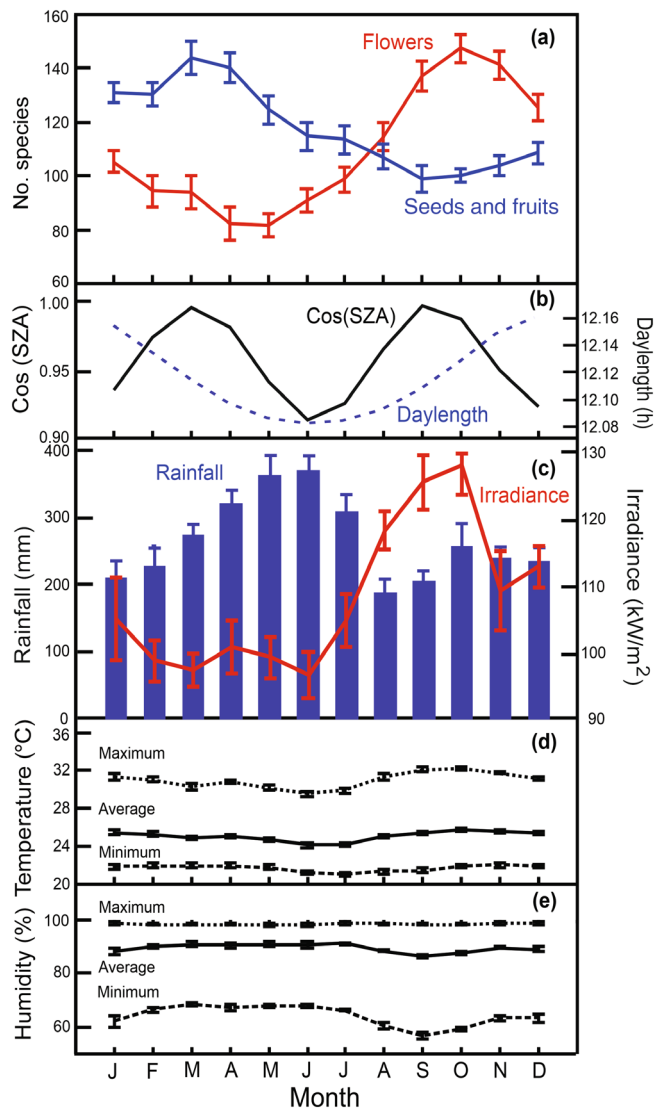
FIGURE 2 Monthly phenology and environmental averages for Yasuní from February 2000 to February 2018. (a) Mean (±SE) number of species present in all 200 traps with flowers (red) and seeds and/or fruits (blue) per month. (b) Cos(solar zenith angle [SZA]) and daylength (solid and dotted lines, respectively); mean of years 2000, 2009 and 2017 using the midpoint of each month (the SD is ≤0.0007 and ≤0.003, respectively, and not shown). (c) Total monthly irradiance (red) and total monthly rainfall (blue); mean ± SE, $N = 11–16$ annual measures for irradiance in each month, $N = 11–15$ values for rainfall. (d) Mean ± SE monthly temperatures: average (solid line), minimum (dashed line) and maximum (dotted line); $N = 11–15$. (e) Mean ± SE monthly relative humidity: average (solid line), minimum (dashed line) and maximum (dotted line); mean, $N = 6–9$ annual values per month, 2008–2018.

overlapping the period identified in the community analysis (March–April; Figure 2a). Patterns in these temporal distributions did not change qualitatively with different minimum sample sizes, indicating patterns were not simply due to differences in commonness or rarity among species in this hyperdiverse forest (see Appendix S1: Figures S17 and S18).

The distribution of vector angles (Figure 3b,e) was significantly different from a uniform distribution but not significantly different from the circular normal distribution (Appendix S1: Table S4), indicating that there was a single unimodal community peak in both flowering and fruiting. The community mean vector angle (i.e., the mean of species-level mean dates of reproduction, whose angles are shown in Figure 3b,e, weighing all species mean vectors equally) for flowering fell in October and that for fruiting in March (Appendix S1: Table S4). These community mean vector angles fell within the peak periods identified in the species-count community (Figure 2a) and the individual species vector (Figure 3b,e) analyses described above (i.e., August–November for flowering and February–April for fruiting).

The phenological activity was not uniformly distributed throughout the year for the overwhelming majority of species (93% for flowering, 97% for fruiting), indicating some degree of intraspecific seasonality (Figure 3; Appendix S1: Table S4; Figures S17 and S18). Of these nonuniformly distributed species, about half fitted a circular normal distribution (47% for flowering, 50% for fruiting; Appendix S1: Table S4), indicating a unimodal seasonal intraspecific peak in reproduction. The remaining species with nonuniform but nonnormal distributions must have had more complex distributions (e.g., irregular, bimodal, multimodal, or unimodal with skewness, or kurtosis). About half of the species in this group had vector lengths >0.5, which usually indicates a unimodal distribution (Morellato et al., 2010). Thus, roughly three-quarters of species were likely to have had unimodal seasonal distributions of flowering and fruiting. Both groups (circular normal and nonuniform/noncircular normal) had similar mean vectors (angles and lengths) to that of the overall community mean vector (Appendix S1: Table S4), indicating a high degree of seasonality in the community. In the cross-correlation analysis of monthly numbers of species flowering and fruiting over 18 years, the maximum correlations (+0.631 to +0.728) occurred at lags of +4–6 months, indicating that flowering led fruiting by 4–6 months (Appendix S1: Figure S3C). A similar lag was seen between the community-level peaks of flowering and fruiting in terms of the mean number of species per month (Figure 2a) and the distribution of vector angles (Figure 3b,e). Fruit development times of individual species, calculated as the time between the flowering and fruiting vector angles of each species, were mostly 2–6 months ($N = 145$ species; Appendix S1: Figure S19). The lower values (≤3 months) were predominantly species flowering in
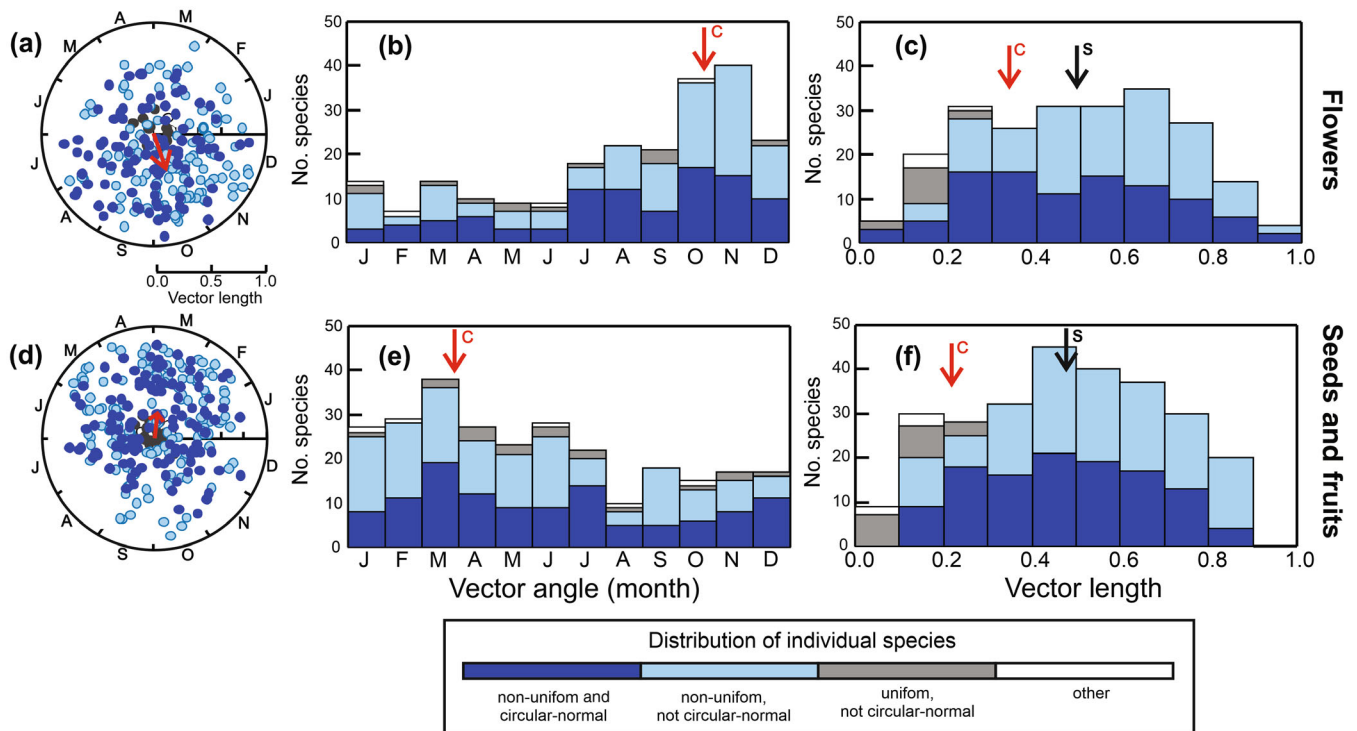
FIGURE 3 (a) Polar graph of flowering vectors ($N = 224$ species with ≥ 50 records and found in ≥ 5 traps) with angle (month) along perimeter and vector length along radii (0.0–1.0). (b) The distribution of vector angles in each month. (c) Distribution of vector lengths. (d–f) Similar polar graphs and distribution for species with seeds and fruit ($N = 271$). Colors denote four nonoverlapping groups of species with distributions determined by the Kuiper (circular normal/nonnormal) and Rayleigh tests (uniform/nonuniform). Dark blue: nonuniform/circular normal distributions; light blue: nonuniform/nonnormal distributions; gray: uniform/nonnormal distributions; and white: other. The red arrows, marked c in (b), (c) and (e), (f), denotes the position of the community-level reproductive vector. The black arrows, marked s in (c, f), denote the arithmetic mean of the vector angles.

December–May, after the peak in flowering and nearer the peak in fruiting.

Annual seasonality in irradiance and rainfall at Yasuní

We observed consistent and predictable seasonality in several environmental variables over 18 years that was probably a key driver of plant community-level phenology (Figure 2). We observed only one peak in irradiance in September–October (128 ± 4.5 kW/m^2 [mean $\pm$ SE, $N = 12$ years] in October; Figure 2c) near the autumnal equinox (Figure 2b), which was ~30% higher than the lows seen from February to June (97 ± 4.0 kW/m^2 in June, Figure 2c). There was no similar peak in irradiance in March and April around the spring equinox, likely caused by higher cloudiness associated with the higher rainfall in this period (as seen in the CRU TS4.04 satellite data; Appendix S1: Figure S10A). Despite no month having <100 mm mean rainfall, rainfall at Yasuní was almost double in May–June (367 ± 24 mm [mean $\pm$ SE,

$N = 14$ years] in June) compared with August–September (186 ± 20 mm [$N = 11$ years] in August). There was also a secondary lower peak in rainfall in October. Periods of high irradiance were accompanied by higher mean and maximum temperatures and lower mean and minimum humidity, while average minimum temperatures and maximum humidity varied minimally through the year (Figure 2d,e).

Most variables in our 18-year climate time series at Yasuní showed strong annual patterns, with significant positive autocorrelations at a 12-month lag (Appendix S1: Figures S6 and S7; $r = 0.494$ for irradiance; $r = 0.350$ for rainfall; $r = 0.411$ for mean temperature; and $r = 0.376$ for mean humidity), as well as at 24- and 36-month lags, indicating consistent annual periodicity. Only maximum humidity lacked significant annual autocorrelations (Appendix S1: Figure S7E). Most climate variables were highly correlated (Appendix S1: Table S1), as expected. Irradiance and mean temperature were strongly negatively correlated with current rainfall ($r = -0.31$ and -0.41, respectively), while mean humidity was most positively correlated with current rainfall ($r = 0.25$).

Cross-correlations of irradiance, mean temperature and mean humidity with rainfall were highest for current rainfall (lag = 0 months), but also significant for 12- and 24-month lags (Appendix S1: Figure S8), indicating strong annual periodicity.

The rainfall seasonality observed at Yasuní was also consistent with patterns in 14 long-term climate datasets from elsewhere in Ecuador east of the Andes. All four lowland sites (185–235 masl), near and including Yasuní (232 masl), were ever-wet (all months received ≥100 mm rainfall) and had annual rainfall of ~3000 mm (Appendix S1: Figure S9). The other 10 meteorological stations in eastern Ecuador are at higher elevations (345–1110 masl) than Yasuní; these had considerably higher annual rainfall, mostly >4000 mm (except for the three southernmost sites) and were also ever-wet. Most of the eastern Ecuador sites had a peak in rainfall in March–May, and many sites had a second lower peak in September–November as seen at Yasuní (Appendix S1: Figure S9).

The modeled satellite-based CRU Ts 4.04 data were significantly correlated with data from Yasuní for rainfall ($r = 0.43$, $p < 0.0001$, $N = 162$ months that have data from both sources, February 2000 to February 2018) and mean, minimum and maximum temperature ($r = 0.55$, $r = 0.47$, $r = 0.56$, respectively, $p < 0.0001$ for all, $N = 156$ months), but the CRU data substantially overestimated mean and maximum temperatures, underestimated minimum temperatures, and did not show any rainfall <200 mm/month (Appendix S1: Figures S11 and S12). Nevertheless, these data provide qualitative insights into the seasonal relationships of climate variables that we did not measure, such as cloudiness, vapor pressure and evapotranspiration (Appendix S1: Figure S10).

Community-level phenology is correlated with climate variation at Yasuní

Supporting our hypothesis that reproductive activity tracks irradiance available to the forest canopy, we found significant relationships between the seasonality of community-level flowering and fruiting and the seasonality of climate variables at Yasuní. Specifically, community-level flowering (mean number of species per month) was greatest during the period of high irradiance (September–November) and lowest during the period of low irradiance (April–May; Figure 2a,c). The number of species flowering at Yasuní was positively cross-correlated with current or recent past irradiance (lag = 0 and 1 month, $r = 0.40$ and 0.46, respectively; Appendix S1: Figure S13), but was also more weakly negatively correlated with current rainfall (Appendix S1:

Figure S13; lag = 0, $r = -0.22$). In contrast with flowering, the number of species fruiting was negatively cross-correlated with current or near future irradiance (Appendix S1: Figure S13; lag = 0 or −1 month, $r = -0.39$ or −0.42, respectively), and more weakly positively correlated with future rainfall (Appendix S1: Figure S13; lags = −1 to −3 months, $r = 0.29$ to 0.22). Because fruiting follows flowering at 4–6 month lags (Figure 2a; Appendix S1: Figure S19) it is also positively correlated with irradiance at 4–6 month lags ($r = 0. 218$ to $r = 0.333$, respectively). Flowering and fruiting also show sizable and significant cross-correlations with mean temperature and mean humidity (Appendix S1: Figure S14) and daylength (Appendix S1: Figure S15A,B), but are weakly correlated with cos(SZA) (Appendix S1: Figure S15C,D), our estimate of the seasonality of top-of-atmosphere irradiance. (See Appendix S1: Section S4 for correlation coefficients of select time lags.)

At the species level, the flower vector angles of more species fell in the periods of highest and intermediate irradiance (August–January) than at other times (Appendix S1: Table S5), supporting our hypothesis that irradiance is driving reproduction. However, fewer species than expected fruited in this period, and fewer species than expected were midway through fruit development in this period. (Results were similar if we used only species with significantly nonuniform distributions; 208 and 264 species for flowering and fruiting, respectively.)

DISCUSSION

Eighteen years of phenological observations, community analysis of >1500 plant species and species-specific vector analyses of >500 species, combined with parallel monitoring of environmental variables, revealed significant annual seasonality in reproductive activity and potential climate drivers in the hyperdiverse ever-wet tropical lowland rain forest of Yasuní. That the forests of the northwestern Amazon lack a distinct dry season has led to the perception that there is small intra-annual variation of importance in major environmental variables. In contrast, we found distinct seasonality in flowering and fruiting, and in irradiance, rainfall, temperature, and humidity. Community-level flowering clearly tracked variation in irradiance. As the climate of Yasuní is similar to that elsewhere in northwestern Amazonía (Appendix S1: Figure S9), our results are likely to apply regionally as well as locally. For example, the Tiputini Biological Station lies ~30 km east of Yasuní and has similar annual rainfall and temperature patterns to Yasuní (Appendix S1: Figure S9), suggesting similar annual variation in irradiance. Also, like Yasuní, Tiputini has a peak

in fruit production in February–March associated with high rainfall (Snodderly et al., 2019), although this study measured reproduction differently than we did and sampled only fleshy-fruited animal-dispersed species.

There are few other long-term studies in ever-wet forests with which to compare our results. Most Neotropical phenology datasets are from clearly seasonal forests, most are <2 years, and few studies measured irradiance (Mendoza et al., 2017). The most comparable Neotropical site, because it uses the same methods, is Luquillo (18° N) in Puerto Rico (Zimmerman et al., 2007). Like Yasuní, Luquillo is ever-wet, but it has slightly higher annual rainfall (3500 mm) and lower floristic diversity. Luquillo has a broad annual peak in irradiance around the summer solstice (May–July), and flowering also peaks during this period.

The potential limits on (and cues for) phenology in equatorial forests such as Yasuní are weaker than in more seasonal or northern forests: variation in daylength is minimal throughout the year (~9 min) and there is no regular dry season. Weaker did not mean inconsequential, however: rainfall and irradiance, as well as temperature and humidity, are highly seasonal. The wettest month receives about twice the rainfall of the driest month, and the month of peak top-of-forest irradiance receives 30% more light than the month with the lowest irradiance.

At Yasuní, flowering at the community level peaks in the period of highest top-of-forest irradiance, with fruiting following ~6 months later and peaking just before the period of highest rainfall. As irradiance fueling photosynthesis is the energy source for plant reproduction, we interpret this pattern as evidence that top-of-forest irradiance is driving the flowering phenology of this community. With these data alone, however, we cannot rule out that high rainfall might physically limit pollination, perhaps by depressing pollinator activity. We are only beginning to understand the specific cues for reproduction in seasonal forests in Central America (Wright et al., 2019; Wright & Calderón, 2018) and in the supra-annual general flowering of Southeast Asia (Chen et al., 2018). Detailed, long-term records of multiple potential environmental cues and drivers of phenology as well as mechanistic gene expression studies (Yeoh et al., 2017) will be crucial to generalizing our understanding across forest types.

Top-of-forest irradiance is a key driver of reproductive phenology

Top-of-forest irradiance is emerging as a primary driver of reproduction in tropical forests (Bendix et al., 2006; Chapman et al., 2018; Hamann, 2004; Wright & Calderón, 2006; Zimmerman et al., 2007), as predicted by van Schaik et al. (1993) and Wright and van Schaik (1994). Indeed, experimental augmentation of irradiance to canopy trees demonstrated that light appears to limit carbon assimilation and fruit production in at least one species of canopy tree during the rainy season (Graham, 2003). Yet, only three of 97 analyses of long-term phenological studies in rainforests (and only four in 39 studies of seasonal or dry tropical forests) in the Neotropics measured irradiance (Mendoza et al., 2017). Over much of the eastern Amazon rainforest, surface irradiance is in phase with, or leads to, forest greening (leaf flushing), but rainfall lags behind greening (Bradley et al., 2011). The signal is less clear in the northwestern Amazon, but irradiance appears to be in phase with greening and unrelated to rainfall (Bradley et al., 2011). Further evidence of the role of irradiance is likely to accumulate, and we echo the emphasis of a recent phenology review (Mendoza et al., 2017) on the importance of measuring irradiance as key to our understanding of plant reproduction.

While irradiance appears to be the major driver of flowering phenology in the ever-wet forests of Yasuní, not all species flowered during the peak in irradiance. The constraints selecting for flowering at what appear to be energetically suboptimal times are presently unknown. Lack of water is unlikely to limit reproduction or growth in this equatorial ever-wet forest, although too much standing water in low-lying areas might do so, and too much rain might limit pollination. Nonetheless, the year-long reproductive season is likely to permit greater opportunities for phenological niche differentiation in reproduction, contributing to the maintenance of forest diversity (Usinowicz et al., 2017).

There is a pronounced peak in the production of mature fruits and seeds in March–April, which is a period of low irradiance at Yasuní, and is several months after peak flowering. This timing may reflect the average time needed to develop and ripen fruits before dispersal. Most of the energy for fruit production is needed after fertilization but before fruits are finally mature and seeds are dispersed. To estimate when energy needs were greatest, we calculated the midpoint of fruit development time as the midpoint between mean vector angles of flowering and fruiting. The midpoint of fruit development time of most species fell in months with relatively high top-of-forest irradiance (November–January; Appendix S1: Table S5). If fruits develop quickly to full size, most development would occur in the period of peak irradiance (August–October) or the following energy-rich months (November–January), supporting the hypothesis that reproduction is limited by light. If fruits develop slowly, the energy needed for fruit growth and development must either accumulate more slowly over longer time periods or come from reserves

stored from the period of maximum irradiance. Without knowledge of fruit development dynamics, it is impossible to choose between these two scenarios. In either case, compared with seeds dispersed soon after flowering, delays of 5–6 months (Appendix S1: Figure S19) between fertilization and dispersal carry other costs that have yet to be explored at Yasuní. These costs might include increased predispersal seed predation, countered by increased chemical or mechanical protection of fruit and seeds, or increased herbivory on stored energy reserves.

The timing of fruit production and seed dispersal might also reflect constraints on the other life history stages, especially seed germination and seedling establishment. In an ever-wet forest in India, seed dormancy delayed germination through the wettest part of the year when the waterlogged soil was a poor germination substrate (Aiyar, 1932). In seasonally dry forests, most species germinate early in the rainy season, which maximizes the length of the first growing season (Chapman et al., 2018; Escobar et al., 2018; Garwood, 1983). For example, on Barro Colorado Island (BCI), Panama, most species fruit during the dry season and germinate quickly with the onset of the rains; many species that fruit later in the rainy season have dormant seeds that delay germination until the beginning of the next rainy season (Garwood, 1983). The majority of species on BCI flower then fruit during the 4-month-long dry season, with both phenophases utilizing the period of maximum irradiance (Zimmerman et al., 2007). Constraints on the timing of seed germination on BCI or elsewhere may reinforce the selection for reproduction during the period of highest irradiance or other beneficial conditions, thereby selecting for particular fruit maturation times (Williamson & Ickes, 2002). At Yasuní, a preliminary 2-year study found no seasonal peak in seedling emergence (Persson, 2005). This timing suggests that conditions for seed germination and seedling establishment are adequate throughout the year (neither too wet nor too dry), and that these stages of the life cycle do not constrain the time of fruit maturation and/or seed dispersal. Without this added constraint, fruit maturation and seed dispersal need not occur soon after flowering, and species might vary in the time required for fruit and seed development. That the fruiting peak is broader than the flowering peak (Figure 2), and the minimum number of species producing fruits per month is higher than for flowering, also suggests fewer constraints on the seasonal timing of fruit production compared with flowering.

Neither rainfall nor irradiance appeared to explain the timing of peak fruit maturity and seed dispersal at Yasuní. Climatic factors such as wind, and biological factors such as lifeforms, phylogeny, seed sizes, dispersal modes, functional traits, or seed germination and seedling emergence may explain variation in fruiting phenology. Analyses contrasting species that reproduce during peak times with those reproducing outside those peaks are also needed.

Predictable seasonality and climate drivers

We expect most northwestern Amazonian forests previously described as "aseasonal" will, in fact, have seasonality in precipitation and top-of-forest irradiance that is strong enough to drive the phenology (and other responses) of the plants that inhabit this region, as we have demonstrated at Yasuní. Our findings of a single community peak in flowering (Figure 2b), strongly correlated with a single peak in top-of-forest irradiance, is consistent with the hypothesis that top-of-forest irradiance is the primary driver of phenology (van Schaik et al., 1993; Wright & van Schaik, 1994; Yeang, 2007a). Our findings are not consistent with the Borchert hypothesis (Borchert et al., 2005, 2015; Calle et al., 2010) that predicts two flowering peaks in equatorial forests, corresponding to the two periods of greatest change in sunrise and sunset or the two peaks in top-of-atmosphere irradiance, which they posit are the only predictable environmental factors at equatorial latitudes. How plants would measure subtle changes in the timing of sunrise/sunset or top-of-atmosphere irradiance is unclear, although plants have a diverse array of wavelength-sensitive photoreceptors that might detect quantitative or qualitative seasonal changes in irradiance reaching their leaves (Yeang, 2007b). As interannual variation in top-of-forest irradiance is clearly higher than variation in daylength, sunrise, or top-of-atmosphere irradiance, current irradiance might also be a better predictor of future environmental conditions than predictable but nearly constant variables such as daylength.

Our ability to predict how climate change will impact the seasonality of reproduction depends on understanding the determinants of the local climate. We had expected two annual peaks in top-of-forest irradiance at Yasuní during the equinoxes (Figure 2b), and hence two peaks in flowering, but found only one around the September equinox. The region is cloudiest from March to June, with cloudiness increasing before rainfall (Appendix S1: Figure S10). While higher cloudiness accounts for the lack of a peak in irradiance at the March equinox (Figure 2c; Appendix S1: Figure S10), the causes of these seasonal differences are unknown. Local rainfall can vary widely over short distances due to the interplay between topography, prevailing winds, and other regional and continental-scale drivers (Espinoza Villar et al., 2015; Killeen et al., 2007). Further integration is needed between on-site measurements of irradiance and other variables and remotely sensed estimates of

cloudiness and atmospheric vapor pressure to understand how much of Yasuní's climate is driven by what is happening nearby in the Andes, or elsewhere in the Amazon, and how much arises from local transpiration dynamics (Sheil & Murdiyarso, 2009).

The 18-year phenology record also documents considerable interannual variation in reproduction at the community level (Figure 1) and in climate (Appendix S1: Figure S5) at Yasuní. Our ability to predict the effects of climate change on phenology in equatorial forests is limited because the regional- and continental-scale drivers of interannual and long-term variation in climate are poorly understood. The Intertropical Convergence Zone (ITCZ) does not appear to have a strong annual effect in this region: on average it reaches its maximum southern extent in January above the Colombian–Ecuadorian border, although it plunges deep (15° S) into South America farther east at that time (Yan, 2005). Northward displacement of the ITCZ causes large interannual variation in rainfall, but mostly in the eastern Amazon (Panisset et al., 2018). The El Niño-Southern Oscillation (ENSO) strongly affects interannual reproduction in the seasonal forest of Panama (Wright & Calderón, 2006) and the dipterocarp forests of Southeast Asia (Ashton et al., 1988; Chechina & Hamann, 2019). In Ecuador, ENSO drives interannual variation in rainfall in the western lowlands and foothills, but not in the inter-Andean valleys or eastern slopes and lowlands (Rossel & Cadier, 2009; Vicente-Serrano et al., 2017), so its potential effects on reproduction at Yasuní might be minimal. The Northern Atlantic Oscillation (NAO) also drives interannual climate variation in Amazonía (Yoon & Zeng, 2010), but its effect in eastern Ecuador and Yasuní is unknown. Satellite imagery and remotely sensed data showed mixed impacts at Yasuní of the mega-droughts in Amazonía in 2005, 2010, and 2015, caused by varied interactions between ENSO and the displacement of the ITCZ (Panisset et al., 2018). Satellite data provide broad coverage, but this is often imprecise at local scales (see Appendix S1: Section S3.5, Figures S11 and S12). This imprecision stresses the importance of expanding the long-term climate data from Yasuní and the region, especially for predicting the effects of climate change on these hyperdiverse forests. In general, the availability of long-term climate data from ever-wet forests is almost as rare as long-term phenology data (Mendoza et al., 2017; Morellato et al., 2013).

Conclusions

We have demonstrated strong seasonality in flowering and fruiting phenology and climate in a hyperdiverse forest in Ecuador long referred to as "aseasonal." Irradiance appears to be the main factor driving seasonality of flowering, in that more species flower during the period of peak irradiance than at other times. These species maximize the energy available for flower production and early fruit and seed development. The peak in fruit maturity and seed dispersal occurs 5–6 months later, during a period of low irradiance but before the peak in annual rainfall. The advantage of fruiting during this peak, if any, is still unclear. Furthermore, large numbers of species reproduce throughout the year outside these peaks. Understanding the climatic or biological drivers of phenology for these species, and the cues all species use to time reproduction, will require further analyses of this unique long-term dataset.

CONFLICT OF INTEREST STATEMENT

The authors declare no conflicts of interest.

DATA AVAILABILITY STATEMENT

Phenology data and monthly climate data collected at the field site (Garwood et al., 2023) are available in the Environmental Data Initiative (EDI) Data Portal: https://doi.org/10.6073/pasta/5e6cb3d7ff741fd9d21965c4a904bc1f. Meteorological data from other Amazonian regions of Ecuador were obtained from the following, as described in Appendix S1: Section S3.4: The Instituto Nacional de Meteorológico e Hidrológico of Servicio Meteorológico e Hidrológico Nacional del Ecuador (INAMHI); University of East Anglia Climatic Research Unit, et al. (2020); Snodderly et al. (2019). To calculate solar data at our research site, spreadsheets from the Global Monitoring Laboratory, Earth System Research Laboratories of the National Oceanic and Atmospheric Administration (NOAA) were used; spreadsheets were obtained from https://www.esrl.noaa.gov/gmd/grad/solcalc/calcdetails.html.

ORCID

Margaret R. Metz https://orcid.org/0000-0002-4221-7318

Simon A. Queenborough https://orcid.org/0000-0002-2468-0958

S. Joseph Wright https://orcid.org/0000-0003-4260-5676

David F. R. P. Burslem https://orcid.org/0000-0001-6033-0990

Renato Valencia https://orcid.org/0000-0001-9770-6568

REFERENCES

Aiyar, T. V. V. 1932. "The Sholas of the Palghat Division, a Study in the Ecology and Silviculture of the Tropical Rain-Forests of Western Ghats." *Indian Forester* 58: 414–432.

Anderson-Teixeira, K., B. Gonzalez, ForestGEO, I. McGregor, E. Gonzalez-Akre, R. Helcoski, V. Herrmann, A. Y. Kim, A. Terrell, and camerondow35. 2020. "forestgeo/Climate: Initial Release." Zenodo. https://zenodo.org/record/4041609.

Ashton, P. S., T. J. Givnish, and S. Appanah. 1988. "Staggered Flowering in the Dipterocarpaceae: New Insights into Floral Induction and the Evolution of Mast Fruiting in the Aseasonal Tropics." *The American Naturalist* 132: 44–66.

Batschelet, E. 1981. *Circular Statistics in Biology*. London: Academic Press.

Bendix, J., J. Homeier, E. Cueva Ortiz, P. Emck, S.-W. Breckle, M. Richter, and E. Beck. 2006. "Seasonality of Weather and Tree Phenology in a Tropical Evergreen Mountain Rain Forest." *International Journal of Biometeorology* 50: 370–384.

Borchert, R., Z. Calle, A. H. Strahler, A. Baertschi, R. E. Magill, J. S. Broadhead, J. Kamau, J. Njoroge, and C. Muthuri. 2015. "Insolation and Photoperiodic Control of Tree Development near the Equator." *New Phytologist* 205: 7–13.

Borchert, R., S. S. Renner, Z. Calle, D. Navarrete, A. Tye, L. Gautier, R. Spichiger, and P. von Hildebrand. 2005. "Photoperiodic Induction of Synchronous Flowering near the Equator." *Nature* 433: 627–29.

Bradley, A. V., F. F. Gerard, N. Barbier, G. P. Weedon, L. O. Anderson, C. Huntingford, L. E. O. C. Aragão, P. Zelazowski, and E. Arai. 2011. "Relationships between Phenology, Radiation and Precipitation in the Amazon Region." *Global Change Biology* 17: 2245–60.

Calle, Z., B. O. Schlumpberger, L. Piedrahita, A. Leftin, S. A. Hammer, A. Tye, and R. Borchert. 2010. "Seasonal Variation in Daily Insolation Induces Synchronous Bud Break and Flowering in the Tropics." *Trees-Structure and Function* 24: 865–877.

Chang-Yang, C. H., C. L. Lu, I. F. Sun, and C. F. Hsieh. 2013. "Flowering and Fruiting Patterns in a Subtropical Rain Forest, Taiwan." *Biotropica* 45: 165–174.

Chapman, C. A., K. Valenta, T. R. Bonnell, K. A. Brown, and L. J. Chapman. 2018. "Solar Radiation and ENSO Predict Fruiting Phenology Patterns in a 15-Year Record from Kibale National Park, Uganda." *Biotropica* 50: 384–395.

Chechina, M., and A. Hamann. 2019. "Climatic Drivers of Dipterocarp Mass-Flowering in South-East Asia." *Journal of Tropical Ecology* 35: 108–117.

Chen, L., L. S. Comita, S. J. Wright, N. G. Swenson, J. K. Zimmerman, X. Mi, Z. Hao, et al. 2018. "Forest Tree Neighborhoods Are Structured More by Negative Conspecific Density Dependence than by Interactions among Closely Related Species." *Ecography* 41: 1114–23.

Delpierre, N., Y. Vitasse, I. Chuine, J. Guillemot, S. Bazot, T. Rutishauser, and C. B. K. Rathgeber. 2016. "Temperate and Boreal Forest Tree Phenology: From Organ-Scale Processes to Terrestrial Ecosystem Models." *Annals of Forest Science* 73: 5–25.

Escobar, D. F. E., F. A. O. Silveira, and L. P. C. Morellato. 2018. "Timing of Seed Dispersal and Seed Dormancy in Brazilian Savanna: Two Solutions to Face Seasonality." *Annals of Botany* 121: 1197–1209.

Espinoza Villar, J. C., S. Chavez, J. Ronchail, C. Junquas, K. Takahashi, and W. Lavado. 2015. "Rainfall Hotspots over the Southern Tropical Andes: Spatial Distribution, Rainfall Intensity, and Relations with Large-Scale Atmospheric Circulation." *Water Resources Research* 51: 3459–75.

Espinoza Villar, J. C., J. Ronchail, J. L. Guyot, G. Cochonneau, F. Naziano, W. Lavado, E. De Oliveira, R. Pombosa, and P. Vauchel. 2009. "Spatio-Temporal Rainfall Variability in the Amazon Basin Countries (Brazil, Peru, Bolivia, Colombia, and Ecuador)." *International Journal of Climatology* 29: 1574–94.

Garwood, N. C. 1983. "Seed Germination in a Seasonal Tropical Forest in Panama: A Community Study." *Ecological Monographs* 53: 159–181.

Garwood, N. C., S. J. Wright, R. Valencia, and M. R. Metz. 2023. "Rainforest Phenology: Flower, Fruit and Seed Production from Biweekly Collections of 200 Traps in the Yasuní Forest Dynamics Plot, Ecuador, 2000–2018 ver 1." Environmental Data Initiative. https://doi.org/10.6073/pasta/5e6cb3d7ff741fd9d21965c4a904bc1f.

Graham, M. H. 2003. "Confronting Multicollinearity in Ecological Multiple Regression." *Ecology* 84: 2809–15.

Hamann, A. 2004. "Flowering and Fruiting Phenology of a Philippine Submontane Rain Forest: Climatic Factors as Proximate and Ultimate Causes." *Journal of Ecology* 92: 24–31.

Harris, I., T. J. Osborn, P. Jones, and D. Lister. 2020. "Version 4 of the CRU TS Monthly High-Resolution Gridded Multivariate Climate Dataset." *Scientific Data* 7: 109.

Hartmann, D. L. 2015. *Global Physical Climatology*. Boston: Newnes.

Hogan, J. A., S. M. McMahon, V. Buzzard, S. T. Michaletz, B. J. Enquist, J. Thompson, N. G. Swenson, and J. K. Zimmerman. 2019. "Drought and the Interannual Variability of Stem Growth in an Aseasonal, Everwet Forest." *Biotropica* 51: 139–154.

Huete, A. R., K. Didan, Y. E. Shimabukuro, P. Ratana, S. R. Saleska, L. R. Hutyra, W. Yang, R. R. Nemani, and R. Myneni. 2006. "Amazon Rainforests Green-Up with Sunlight in Dry Season." *Geophysical Research Letters* 33: L06405.

Killeen, T. J., M. Douglas, T. Consiglio, P. M. Jørgensen, and J. Mejia. 2007. "Dry Spots and Wet Spots in the Andean Hotspot." *Journal of Biogeography* 34: 1357–73.

Kovach, W. 1994, 2013. *Oriana*. Wales: Kovach Computing Services.

Leigh, E. G., A. S. Rand, and D. M. Windsor. 1985. *The Ecology of a Tropical Forest: Seasonal Rhythms and Long-Term Changes*. Washington: Smithsonian Institution Press.

Leigh, E. G., Jr. 2004. "How Wet Are the Wet Tropics?" In *Tropical Forest Diversity and Dynamism: Findings from a Large-Scale Plot Network*, edited by E. C. Loso and E. G. Leigh, Jr., 43–55. Chicago: University of Chicago Press.

McGregor, G. R., and S. Nieuwolt. 1998. *Tropical Climatology: An Introduction to the Climates of the Low Latitudes*, 2nd ed. Hoboken: John Wiley & Sons, Ltd.

Mendoza, I., C. A. Peres, and L. P. C. Morellato. 2017. "Continental-Scale Patterns and Climatic Drivers of Fruiting Phenology: A Quantitative Neotropical Review." *Global and Planetary Change* 148: 227–241.

Morellato, L. P. C., L. F. Alberti, and I. L. Hudson. 2010. "Applications of Circular Statistics in Plant Phenology: A Case Studies Approach." In *Phenological Research: Methods for Environmental and Climate Change Analysis*, edited by I. L. Hudson and M. R. Keatley, 339–359. Dordrecht: Springer.

Morellato, L. P. C., M. G. G. Camargo, and E. Gressler. 2013. "A Review of Plant Phenology in South and Central America." In *Phenology: An Integrative Environmental Science*, edited by M. D. Schwartz, 91–113. Dordrecht: Springer.

Neill, D. A., and P. M. Jørgensen. 1999. In *Climates*, edited by P. M. Jørgensen. St Louis: Missouri Botanical Garden Press.

Netherly, P. J. 1997. "Loma y ribera: Patrones de asentamiento prehistóricos en la Amazonia Ecuatoriana." *Fronteras de Investigación* 1: 33–54.

Panisset, J. S., R. Libonati, C. M. P. Gouveia, F. Machado-Silva, D. A. França, J. R. A. França, and L. F. Peres. 2018. "Contrasting Patterns of the Extreme Drought Episodes of 2005, 2010 and 2015 in the Amazon Basin." *International Journal of Climatology* 38: 1096–1104.

Perez, A., C. Hernández, H. Romero-Saltos, and R. Valencia. 2014. *Árboles Emblemáticos de Yasuní*. Quito: Pontificia Universidad Catolica Del Ecuador.

Persson, V. 2005. "Effects of Climatic Seasonality on Reproductive Phenology of Tropical Forest Plants." PhD diss., University of Aberdeen, Aberdeen.

Pitman, N. C. A. 2000. "A Large-Scale Inventory of Two Amazonian Tree Communities." PhD diss., Duke University, Durham.

Queenborough, S. A., D. F. R. P. Burslem, N. C. Garwood, and R. Valencia. 2007. "Habitat Niche Partitioning by 16 Species of Myristicaceae in Amazonian Ecuador." *Plant Ecology* 192: 193–207.

Reich, P. B. 1995. "Phenology of Tropical Forests: Patterns, Causes, and Consequences." *Canadian Journal of Botany-Revue Canadienne de Botanique* 73: 164–174.

Richards, P. W. 1952. *The Tropical Rain Forest*. Cambridge: Cambridge University Press.

Rohlf, F. J., and R. R. Sokal. 1995. *Statistical Tables*, 3rd ed. New York: W. H. Freeman & Co.

Rossel, F., and E. Cadier. 2009. "El Niño and Prediction of Anomalous Monthly Rainfalls in Ecuador." *Hydrological Processes* 23: 3253–60.

Sheil, D., and D. Murdiyarso. 2009. "How Forests Attract Rain: An Examination of a New Hypothesis." *BioScience* 59: 341–47.

Silman, M. R. 2011. "Plant Species Diversity in Amazonian Forests." In *Tropical Rainforest Responses to Climatic Change*, edited by M. Bush, J. Flenley, and W. Gosling, 285–314. Heidelberg: Springer.

Snodderly, D. M., K. M. Ellis, S. R. Lieberman, A. Link, E. Fernandez-Duque, and A. Di Fiore. 2019. "Initiation of Feeding by Four Sympatric Neotropical Primates (*Ateles belzebuth*, *Lagothrix lagotricha poeppigii*, *Plecturocebus* (*Callicebus*) *discolor*, and *Pithecia aequatorialis*) in Amazonian Ecuador: Relationships to Photic and Ecological Factors." *PLOS ONE* 14: e0210494.

Sokal, R. R., and F. J. Rohlf. 1995. *Biometry: The Principles and Practice of Statistics in Biological Research*, Third ed. New York: Freeman & Company.

Sombroek, W. 2001. "Spatial and Temporal Patterns of Amazon Rainfall: Consequences for the Planning of Agricultural Occupation and the Protection of Primary Forests." *Ambio* 30: 388–396.

Staggemeier, V. G., M. G. G. Camargo, J. A. F. Diniz-Filho, R. Freckleton, L. Jardim, and L. P. C. Morellato. 2020. "The Circular Nature of Recurrent Life Cycle Events: A Test Comparing Tropical and Temperate Phenology." *Journal of Ecology* 108: 393–404.

Systat Software Inc. 2009. Systat, Version 13.1. Palo Alto, CA: Inpixon. https://systatsoftware.com/systat/.

University of East Anglia Climatic Research Unit, I. C. Harris, P. D. Jones, and T. Osborn. 2020. "CRU TS4.04: Climatic Research Unit (CRU) Time-Series (TS) Version 4.04 of High-Resolution Gridded Data of Month-by-Month Variation in Climate (January 1901–December 2019)." Centre for Environmental Data Analysis. https://catalogue.ceda.ac.uk/uuid/89e1e34ec3554dc98594a5732622bce9.

Usinowicz, J., C. H. Chang-Yang, Y.-Y. Chen, J. S. Clark, C. Fletcher, N. C. Garwood, Z. Hao, et al. 2017. "Temporal Coexistence Mechanisms Contribute to the Latitudinal Gradient in Forest Diversity." *Nature* 550: 105–8.

Valencia, R., R. S. Condit, R. B. Foster, K. Romoleroux, G. Villa Muñoz, J.-C. C. Svenning, E. Magard, M. S. Bass, E. C. Losos, and H. Balslev. 2004. "Yasuni Forest Dynamics Plot, Ecuador." In *Tropical Forest Diversity and Dynamism: Findings from a Large-Scale Plot Network*, edited by E. C. Losos and E. G. Leigh, 609–620. Chicago: University of Chicago Press.

Valencia, R., R. S. Condit, K. Romoleroux, R. B. Foster, G. Villa Muñoz, E. C. Losos, H. Balslev, J.-C. C. Svenning, and E. Magard. 2004. "Tree Species Diversity and Distribution in a Forest Plot at Yasuni National Park, Amazonian Ecuador." In *Tropical Forest Diversity and Dynamism: Findings from a Large-Scale Plot Network*, edited by E. C. Losos and E. G. Leigh, 107–118. Chicago: University of Chicago Press.

Valencia, R., R. B. Foster, G. Villa, R. S. Condit, J.-C. C. Svenning, C. Hernández, K. Romoleroux, E. Losos, E. Magard, and H. Balslev. 2004. "Tree Species Distributions and Local Habitat Variation in the Amazon: Large Forest Plot in Eastern Ecuador." *Journal of Ecology* 92: 214–229.

van Schaik, C. P., J. W. Terborgh, and S. J. Wright. 1993. "The Phenology of Tropical Forests: Adaptive Significance and Consequences for Primary Consumers." *Annual Review of Ecology and Systematics* 24: 353–377.

Vicente-Serrano, S. M., E. Aguilar, R. Martínez, N. Martín-Hernández, C. Azorin-Molina, A. Sanchez-Lorenzo, A. El Kenawy, et al. 2017. "The Complex Influence of ENSO on Droughts in Ecuador." *Climate Dynamics* 48: 405–427.

von Humboldt, A. 1850. *Views of Nature: Or Contemplations on the Sublime Phenomena of Creation*. London: Cambridge University Press.

Whitmore, T. C. 1984. *The Tropical Rain Forests of the Far East*. Oxford: Oxford University Press.

Williamson, G. B., and K. Ickes. 2002. "Mast Fruiting and ENSO Cycles: Does the Cue Betray a Cause?" *Oikos* 97: 459–461.

Wright, S. J. 1996. "Phenological Responses to Seasonality in Tropical Forest Plants." In *Tropical Forest Plant Ecophysiology*, edited by S. S. Mulkey, R. L. Chazdon, and A. P. Smith, 440–460. Boston: Springer.

Wright, S. J., and O. Calderón. 1995. "Phylogenetic Patterns among Tropical Flowering Phenologies." *Journal of Ecology* 83: 937–948.

Wright, S. J., and O. Calderón. 2006. "Seasonal, El Niño and Longer Term Changes in Flower and Seed Production in a Moist Tropical Forest." *Ecology Letters* 9: 35–44.

Wright, S. J., and O. Calderón. 2018. "Solar Irradiance as the Proximate Cue for Flowering in a Tropical Moist Forest." *Biotropica* 50: 374–383.

Wright, S. J., O. Calderón, and H. C. Muller-Landau. 2019. "A Phenology Model for Tropical Species that Flower Multiple Times each Year." *Ecological Research* 34: 20–29.

Wright, S. J., and C. P. van Schaik. 1994. "Light and the Phenology of Tropical Trees." *The American Naturalist* 143: 192–99.

Wu, J., K. Guan, M. Hayek, N. Restrepo-Coupe, K. T. Wiedemann, X. Xu, R. Wehr, et al. 2017. "Partitioning Controls on Amazon Forest Photosynthesis between Environmental and Biotic Factors at Hourly to Interannual Timescales." *Global Change Biology* 23: 1240–57.

Xiao, X., S. Hagen, Q. Zhang, M. Keller, and B. Moore. 2006. "Detecting Leaf Phenology of Seasonally Moist Tropical Forests in South America with Multi-Temporal MODIS Images." *Remote Sensing of Environment* 103: 465–473.

Yan, Y. Y. 2005. "Intertropical Convergence Zone (ITCZ)." In *Encyclopedia of World Climatology*, edited by J. E. Oliver. Dordrecht: Springer.

Yeang, H.-Y. 2007a. "Synchronous Flowering of the Rubber Tree (*Hevea brasiliensis*) Induced by High Solar Radiation Intensity." *New Phytologist* 175: 283–89.

Yeang, H.-Y. 2007b. "The Sunshine-Mediated Trigger of Synchronous Flowering in the Tropics: The Rubber Tree as a Study Model." *New Phytologist* 176: 727–730.

Yeoh, S. H., A. Satake, S. Numata, T. Ichie, S. L. Lee, N. Basherudin, N. Muhammad, et al. 2017. "Unravelling Proximate Cues of Mass Flowering in the Tropical Forests of South-East Asia from Gene Expression Analyses." *Molecular Ecology* 26: 5074–85.

Yoon, J.-H., and N. Zeng. 2010. "An Atlantic Influence on Amazon Rainfall." *Climate Dynamics* 34: 249–264.

Zimmerman, J. K., S. J. Wright, O. Calderon, M. A. Pagan, and S. Paton. 2007. "Flowering and Fruiting Phenologies of Seasonal and Aseasonal Neotropical Forests: The Role of Annual Changes in Irradiance." *Journal of Tropical Ecology* 23: 231–251.

SUPPORTING INFORMATION

Additional supporting information can be found online in the Supporting Information section at the end of this article.